NUCLEAR INSTRUMENTS AND METHODS 100 (1972) 493–504; © NORTH-HOLLAND PUBLISHING CO.

PULSE-SHAPING IN LOW-NOISE NUCLEAR AMPLIFIERS: A PHYSICAL APPROACH TO NOISE ANALYSIS

F. S. GOULDING

Lawrence Berkeley Laboratory, University of California, Berkeley, California 94720, U.S.A.

Received 21 December 1971

Analysis of the relative noise performance of many types of pulse-shaping systems is discussed in terms of recent work on noise analysis. The simplicity of the method, and its direct connection to physical processes, is stressed. Applications of the technique to time-variant as well as time-invariant systems are illustrated.

1. Introduction

A very simple approach to the problem of comparing the noise behavior of various pulse-shaping networks used in low-noise nuclear pulse-amplifiers has evolved in the past five years. Notable contributors to this approach include Amsel et al.[1]), Radeka et al.[2,3]), and Deighton[4]). The method rests on an elementary physical picture of noise; as the analysis is carried out completely in the time domain, intuitive comparisons become possible between various pulse-shapes, and the effects of changing parameters can readily be calculated. Furthermore, the range of shaping techniques that can be analyzed is far greater than could conveniently be handled by earlier methods. In particular, shapers containing time-variant elements can be studied.

Unfortunately, the power of the technique has escaped the notice of many physicists and engineers working with pulse-amplifiers. This paper represents an attempt to express the ideas involved in the method simply, while avoiding the specialized terms of information theory, so that a clearer physical picture of the parameters controlling noise emerges.

Various considerations enter into the choice of a pulse-shaping network in a nuclear pulse-amplifier. These include:

1) Signal/noise performance.
2) Counting-rate behavior.
3) Sensitivity to rise-time fluctuations of the input signal.
4) Suitability of the output pulse-shape for feeding a pulse-height analyzer.

The relative emphasis on these various factors should depend on the application. For example, low-energy X-ray spectroscopy using silicon detectors places most emphasis on (1), but (2) can also be very important. However, for large germanium γ-ray detectors used to measure high-energy γ-rays, (1) is less important, as the spectral line-width may depend more on detector charge-production statistics than on electronic noise. In this case, detector signal rise-time fluctuations may be the critical factor. It is therefore important to be able to assess the effect on the signal-to-noise ratio of using a pulse-shaper whose output is rather independent of input signal risetime. To make an optimum choice of pulse-shaper for a given application one must assess the trade-offs among all four factors. No single pulse-shaper is best from all points of view.

2. Noise sources

Fundamental noise sources of at least two types exists in all low-noise nuclear pulse amplifiers, where a very high input impedance is used to match high impedance radiation detectors. The first arises from the discrete electronic nature of any current flowing in the input circuit of the preamplifier. Grid-current in a vacuum tube, gate-current in a field-effect transistor, and leakage-current in a detector all constitute sources of this type. The second fundamental noise type is that due to the discrete electronic nature of the current flowing through the input and later amplifying elements (i.e. later than the input circuit).

Distinction between the two types of noise is made

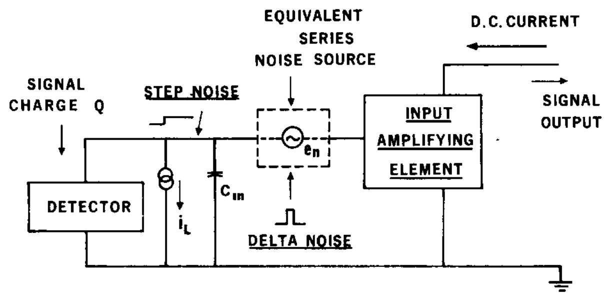

Fig. 1. Fundamental noise sources in a preamplifier.

because the charge due to electron flow in the input circuit is integrated by the input circuit capacitance (including detector), to appear as tiny voltage steps at the input to the preamplifier (see fig. 1). We will call this *STEP NOISE*. On the other hand, flow of an electron through the input amplifying device produces only a short delta pulse of current in the output circuit; an equivalent circuit to represent noise due to this process is a delta-function voltage generator in series with the input circuit. We will call this *DELTA NOISE*. As shown in fig. 1, the two noise sources combine as two randomly varying voltages in series with the input electrode of the amplifying element. One is the summation of a random time-series of steps, while the other is the summation of a similar series of deltas.

For the purpose of this paper we make the following reasonable assumptions:

1) Individual electrons causing each type of noise occur at random times with a mean interval between electrons very much shorter than the pulse-shaping times used in the amplifier. The space-charge smoothing effect in a vacuum tube is one well known reason for deviation from a truly random distribution. Furthermore, input circuit leakage currents below 10^{-14} A are not uncommon, so, in a typical pulse-shaping time (~ 10 μsec), an average of just about a single leakage-current electron will flow in the input circuit. This is certainly not enough to justify the application of normal statistics, but, when averaged over a large number of signal pulses, one might expect to observe the same spectral line-broadening as is predicted by normal statistics. Despite these factors, the spectral line-width in a spectrometer should differ only slightly from the value we calculate.

2) We assume that only step- and delta-noise are present. Many well-known noise sources, including flicker-noise in vacuum tubes, surface-noise in semiconductor components, and excess-noise in resistors, cannot be represented by step- or delta-functions at the amplifier input. The primary noise source in these cases will be equivalent to a step generator coupling to the input circuit via distributed networks. These excess-noise generators, which are virtually impossible to predict, can be made almost negligible by selecting components producing only low levels of excess noise. Our assumption that only step- and delta-noise types are present is then a reasonable approximation to the truth.

3) The discrete noise events at the amplifier input are assumed to correspond to the same amount of charge flow. For step-noise this means that the voltage steps at the input due to leakage-current electrons are all equal. For delta-noise it implies that the delta functions produced by the equivalent noise generator (fig. 1) are all of the same area. This assumption may sometimes be invalid – for example, the thermal generation of a hole-electron pair in a semi-conductor detector produces a charge flow in the external circuit which is the sum of hole- and electron-drift components. If either carrier is trapped for a long time, the prompt noise signal is reduced below its single-electron value. For the purpose of analysis we could separately consider groups of noise pulses, each group having a certain amplitude, the sum their effects on the signal. If the pulses in each group constitute a random time sequence, the same general result will be obtained as is produced by considering only a single group of one size. It therefore appears that this assumption is reasonably valid for the purposes of our analysis.

3. Analysis method

Any calculation of absolute noise levels in an amplifier demands a detailed knowledge of the physical processes involved in the circuit elements. Fortunately, our intention here is to make only a comparative evaluation of the noise performance of various pulse-shapers, and it is not necessary to consider details of the physical processes responsible for causing the noise. We therefore make only the simple assumption that an average number of single-electron step-functions (n_s/sec) and of delta-functions (n_Δ/sec) are produced in the input circuit by the noise sources. The signal from the detector is assumed to be a charge-pulse producing a step-function voltage signal at the input of the preamplifier.

Fig. 2 shows the complete signal processing chain. In time-invariant (passive) pulse-shapers, both signal and noise are processed by a pulse-shaper (sometimes called a noise filter) to produce the best possible signal/noise ratio at the output. We note that, in this case, individual noise steps are shaped by the pulse-shaper in exactly the same way as the signal–indepen-

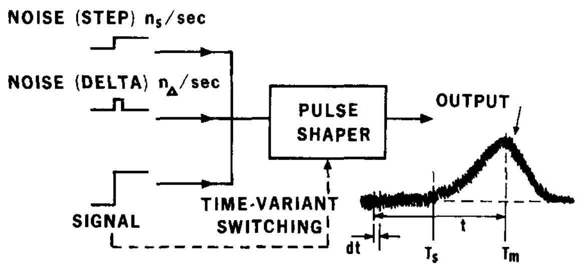

Fig. 2. The basic pulse-shaping system.

dent of the arrival time of the noise step. However, in time-variant systems, where the pulse-shaper elements change value in synchronism with the signal (path shown in dotted line in fig. 2), the effect of the pulse-shaper on noise steps (and deltas) depends on their time of arrival with reference to signal pulses.

In our analysis we assume that the output signal amplitude is measured at a fixed time T_m on the signal. The amplitude measured for a given signal is equal to the true signal amplitude plus (or minus) the cumulative effect of all noise-steps occurring before T_m. To determine this effect we must define a *STEP-NOISE RESIDUAL FUNCTION** $R(t)$ that represents the residual effect at T_m of a single unit-amplitude noise step occurring t seconds prior to T_m. $R(t)$ can be determined analytically if the shaping network parameters are known, or can be measured by injection of a step-function into the system input at variable times earlier than T_m, while measuring the response at T_m.

Now we suppose that unit amplitude noise steps occur at a rate n_s/sec. In any selected short time interval dt, the number of noise steps cannot be predicted, but two things are known about the number:

1) If we count the number N of noise steps occurring in each of many time increments dt, the average of the numbers obtained will be $n_s dt$. Therefore

$$\bar{N} = n_s \mathrm{d}t\,.$$

2) The mean square fluctuation $\langle n^2 \rangle$ in N will be given by:

$$\langle n^2 \rangle = n_s \mathrm{d}t\,.$$

But each noise step in a time increment dt occurring t_1 seconds prior to the measurement time T_m of a signal produces a response $R(t_1)$ at the measurement time. Therefore, if a large number of signals is measured, the mean square effect on the amplitude determination, due to noise in time elements dt occurring t_1 seconds prior to each signal measurement time, is equal to:

$$\langle n^2 \rangle \cdot [R(t_1)]^2 = n_s [R(t_1)]^2 \mathrm{d}t\,.$$

The total mean square effect of all noise steps prior to T_m is obtained by summing the mean square effects for all values of t_1:

Total mean square step noise effect at T_m

$$= n_s \int_0^\infty [R(t)]^2 \mathrm{d}t\,.$$

It will be useful to define a step-noise index that contains only those parameters determined by the pulse-shaper. As n_s is independent of the shaper it will be omitted from the index, but the signal amplitude S (i.e. response to a unit-step input signal), which depends on the shaper, must be included. As the factor of importance is the ratio of mean square noise to the square of signal amplitude, our step-noise index will be defined as:

$$STEP\ NOISE\ \langle N_s^2 \rangle = \frac{1}{S^2} \int_0^\infty [R(t)]^2 \mathrm{d}t\,. \qquad (1)$$

A similar noise index can be developed for delta-noise. Each delta-noise pulse is assumed to be of duration Δt, where Δt is very short compared to any time-constant involved in the pulse-shaper, and the area of the delta is assumed to have a fixed value. These assumptions about the delta-pulse generator of fig. 1 corresponds physically to a single electron flowing through the input amplifying element in a transit-time Δt. The delta-function can be considered as a positive step-function of amplitude proportional to $1/\Delta t$, followed Δt later by a negative step function of the same amplitude. If the noise pulse precedes T_m by t, its effect at T_m will be given by

$$\frac{1}{\Delta t}[R(t) - R(t - \Delta t)]\,.$$

For $\Delta t \to 0$ this function is the differential of $R(t)$, and we can define it as the *DELTA-NOISE RESIDUAL FUNCTION* $R'(t)$. Proceeding exactly as for step-noise, the delta-noise index can be defined as:

$$DELTA\ NOISE\ \langle N_\Delta^2 \rangle = \frac{1}{S^2} \int_0^\infty [R'(t)]^2 \mathrm{d}t\,. \qquad (2)$$

It is important to realize that the entire effect of a pulse-shaper on noise is contained in eqs. (1) and (2). Once $R(t)$ and S are established for various pulse-shapes, evaluation of their relative noise performance is simply a matter of evaluating the indices $\langle N_s^2 \rangle$ and $\langle N_\Delta^2 \rangle$. The fact that $R'(t)$ appears in eq. (2), while $R(t)$ appears in eq. (1), implies that $\langle N_s^2 \rangle$ is always dimensionally different from $\langle N_\Delta^2 \rangle$ by a factor of (time)^2.

4. Examples of method

Discussion of a few simple examples that can be represented graphically will demonstrate the power of the method. These examples will point out a number of general conclusions concerning the noise performance of pulse shapers.

* Radeka[3]) uses the term "Weighting Function".

4.1. Time-invariant trapezoidal pulse-shaper

The example chosen first is a shaper developing the asymmetrical trapezoidal output pulse shown in the top illustration of fig. 3. Circuit details involved in the shaper need not be known except that all components must be linear, and, in this case, time-invariant. Fig. 3 contains a graphical development of the functions required to evaluate the noise indices.

Derivation of the function $R(t)$ is the key step in calculating the noise indices. In this case it is very simply derived by considering the effect at T_m of a unit-step input occurring at t before T_m, then plotting this effect as a function of t. Note that $R(t)$ is the same shape as the signal response in this case. This is always true for time-invariant (passive) shapers, but is never true for time-variant shapers, where the shaping of noise pulses depends on their time relationship to the signal.

Once $R(t)$ is developed, $[R(t)]^2$, $R'(t)$ and $[R'(t)]^2$ are readily derived. The area beneath $[R(t)]^2$, shown in the lower left illustration of fig. 3, determines the step-noise index $\langle N_s^2 \rangle$, since we have normalized to a signal amplitude $S=1$. The area beneath $[R(t)]^2$ is proportional to the total time $\tau_1+\tau_2+\tau_3$ occupied by the pulse, if the ratios τ_1/τ_2 and τ_2/τ_3 are maintained constant. The general conclusion that STEP NOISE is proportional to the pulse time-scale* follows from this simple observation – it applies to all shaping networks.

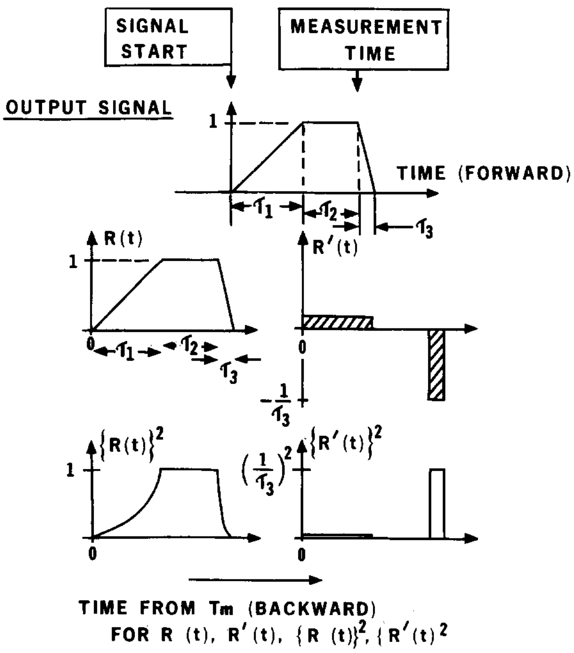

Fig. 3. Time-invariant trapezoidal pulse-shaper.

The DELTA RESIDUAL FUNCTION $R'(t)$ is easily derived from $R(t)$ and is shown in the right half of fig. 3. Since $R(t)$ must return to its baseline, the positive and negative areas of $R'(t)$ must be equal. It follows that the area under $[R'(t)]^2$ in the bottom right illustration is dominated by the τ_3 part of the function. This means that DELTA NOISE is determined largely by the region of the signal-response where the rate-of-change is a maximum. We also note that the flat portion of the signal response contributes *no* delta noise, and that the area under $[R'(t)]^2$ is inversely proportional to the time scale of the signal response.

We have:

STEP NOISE

$$\langle N_s^2 \rangle = \int_0^{\tau_3} \left(\frac{t}{\tau_3}\right)^2 \mathrm{d}t + \int_0^{\tau_2} (1)^2 \,\mathrm{d}t + \int_0^{\tau_1} \left(\frac{t}{\tau_1}\right)^2 \mathrm{d}t$$

$$= \frac{\tau_3}{3} + \tau_2 + \frac{\tau_1}{3} = \tau_2 + \frac{(\tau_1+\tau_3)}{3}\,; \tag{3}$$

DELTA NOISE

$$\langle N_\Delta^2 \rangle = \int_0^{\tau_3} \left(\frac{1}{\tau_3}\right)^2 \mathrm{d}t + \int_0^{\tau_1} \left(\frac{1}{\tau_1}\right)^2 \mathrm{d}t = \frac{1}{\tau_1} + \frac{1}{\tau_3}. \tag{4}$$

Counting-rate considerations usually dictate a maximum duration for the signal (i.e. $\tau_1+\tau_2+\tau_3$ must be smaller than a certain value). Also, the sensitivity of output amplitude to detector signal rise-time is related to the duration τ_2 of the flat-top on the output pulse – the longer τ_2, the less the sensitivity. If we define a maximum signal duration T_s, and demand a flat-top duration T_F, eqs. (3) and (4) show that the best shape is that for which $\tau_1 = \tau_3 = \frac{1}{2}(T_s - T_F)$.

The noise indices are then given by:

$$\langle N_s^2 \rangle = \tfrac{1}{3}(2\,T_F + T_s), \tag{5}$$

$$\langle N_\Delta^2 \rangle = \frac{4}{T_s - T_F}. \tag{6}$$

When we generalize from these conclusions, the following rules are clear:

1) *STEP NOISE* is proportional to the time-scale of the pulse-shape.
2) *DELTA NOISE* is inversely proportional to the time-scale.

* The term "time-scale" will be used in many places in this paper. For a given pulse-shape a change in time-scale implies a proportionate change in all time segments of the pulse-shape.

3) For a fixed total signal duration, best results are achieved by making the pulse shape symmetrical.
4) While a flat region on a signal does not directly contribute to DELTA NOISE, it does result in an increase in the signal rate-of-rise in other portions of the pulse if the total pulse-width is fixed. It thereby indirectly increases DELTA NOISE, as well as affecting STEP NOISE, for a fixed total pulse-width.

4.2. Equal RC integrator–differentiator

The signal (step) response of a pulse shaper containing a single RC differentiator, and an RC integrator with the same RC value, is given by:

$$\text{output} = \frac{t}{\tau_0} \mathrm{e}^{(1-t/\tau_0)},$$

where t is the time, τ_0 is the peaking time, and the peak amplitude is unity (see fig. 4). As in the previous example, $R(t)$ is the same as the signal response.

Proceeding immediately to the noise indices given in eqs. (1) and (2), and normalizing to a signal amplitude $S=1$:

STEP NOISE

$$\langle N_s^2 \rangle = \int_0^\infty \frac{t^2}{\tau_0^2}\, \mathrm{e}^{2(1-t/\tau_0)}\,\mathrm{d}t = \frac{\mathrm{e}^2 \tau_0}{8} \int_0^\infty \left(\frac{2t}{\tau_0}\right)^2 \mathrm{e}^{-2(t/\tau_0)}\,\mathrm{d}\left(\frac{2t}{\tau_0}\right) = \frac{\mathrm{e}^2 \tau_0}{4} = 1.87\,\tau_0 . \tag{7}$$

Also,

$$R'(t) = \mathrm{e}\left[\frac{\mathrm{e}^{-t/\tau_0}}{\tau_0} - \frac{t}{\tau_0^2}\mathrm{e}^{-t/\tau_0}\right].$$

DELTA NOISE

$$\langle N_\Delta^2 \rangle = \frac{\mathrm{e}^2}{\tau_0^2} \int_0^\infty \left[\mathrm{e}^{-2t/\tau_0}\left(1 + \frac{t^2}{\tau_0^2} - 2\frac{t}{\tau_0}\right)\right]\mathrm{d}t = \frac{\mathrm{e}^2}{4\tau_0} = \frac{1.87}{\tau_0}. \tag{8}$$

Eqs. (7) and (8) can be compared directly with eqs. (5) and (6) to show the differences between the RC integrator–differentiator and the trapezoidal shapers. To simplify the comparison, we can make the flat-top (T_F) zero, thereby producing a triangular waveform. If we make $T_s = 2\tau_0$, so that the peak of the triangle occurs at the same time as the peak of the RC shaped pulse, we have:

Triangular shaper
$$\langle N_s^2 \rangle = 0.667\,\tau_0, \qquad \langle N_\Delta^2 \rangle = 2/\tau_0;$$

RC integ. diff.
$$\langle N_s^2 \rangle = 1.87\,\tau_0, \qquad \langle N_\Delta^2 \rangle = 1.87/\tau_0.$$

This shows that the noise index for the symmetrical triangular shape is slightly worse for delta-noise, but much better for step-noise – assuming the same peaking-time. The triangle returns to its baseline much earlier than the other waveform. Optimum choice of the peaking-time of either waveform depends on the relative magnitudes of n_s and n_Δ, which depend on the characteristics of input circuit elements. If n_s is very small, delta-noise tends to be dominant; we can then increase the time-scale for the triangle so that its performance becomes superior to the RC integrator–differentiator both in regard to step- and delta-noise, while also exhibiting better counting-rate performance. Provision of a flat-top results in a trapezoidal shape much superior in regard to lack of sensitivity to detector signal rise-time variations.

These examples illustrate the simplicity of the method as a tool to compare the behavior of very

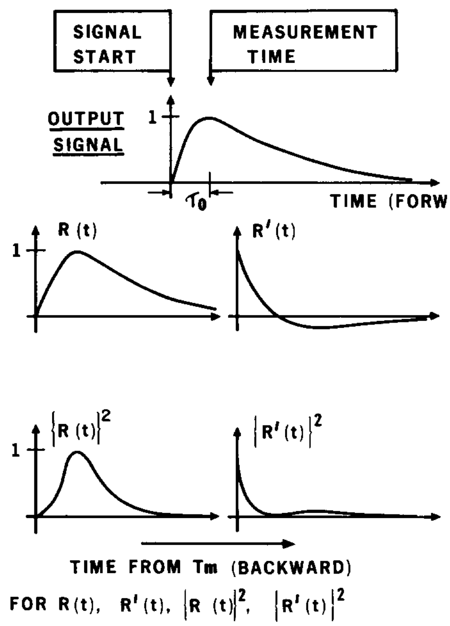

Fig. 4. Equal RC integrator–differentiator.

different time-invariant pulse-shapers. The effects of changes in symmetry of the trapezoid, and in the duration of its flat-top can easily be calculated – this is in contrast to more conventional methods of analysis. The two examples also illustrate the ability of the method to analyze shapers producing waveforms expressible in purely analytical form (4.2), or ones that must be treated by piecewise integration (4.1). We will now examine its application to some time-variant systems of different degrees of complexity.

4.3. Gated-integrator trapezoidal pulse-shaper

This simple time-variant system consists of a shaper (see fig. 5), producing a rectangular pulse of duration T, feeding a gated-integrator switched on at the start of the signal to integrate the rectangular pulse for a time T_I. At the end of T_I, the integrator output is rapidly restored to zero by shorting out the integrating capacitor. The output signal consists of a ramp rising linearly for the time T, followed by a flat-top until the end of the integration period. As pointed out by Radeka[3]), the resulting pulse is insensitive to detector signal rise-time variations as long as they occur in a time smaller than $T_I - T$.

In this case, the step-noise residual function $R(t)$ is not the same as the output signal. The function $R(t)$ is generated by determining the overlapping area of the rectangular pulse of width T with the integration period T_I, for the whole possible range of times between the start of the pulse and measurement time T_m. Graphically, one can imagine sliding the rectangular pulse through the region of integration, then computing the area of intersection between T and T_I for each position of the pulse. We then have:

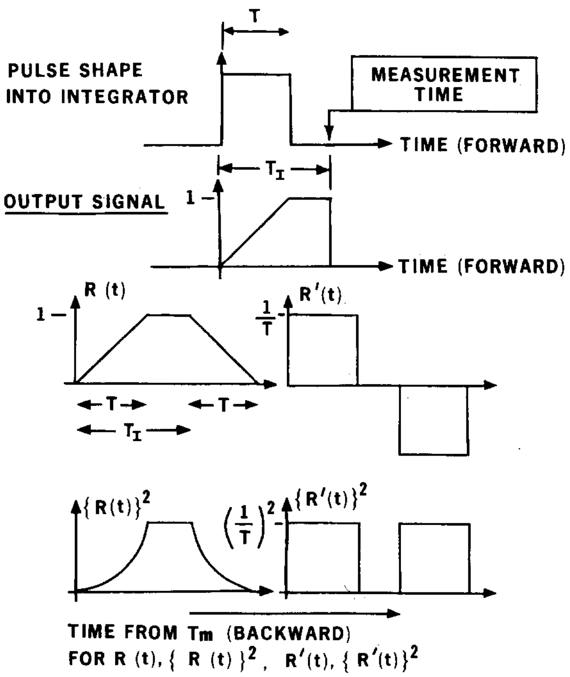

Fig. 5. Gated-integrator trapezoidal pulse-shaper.

STEP NOISE

$$\langle N_s^2 \rangle = \int_0^\infty [R(t)]^2 \, dt = 2\int_0^T \left(\frac{t}{T}\right)^2 dt + \int_0^{T_I - T} (1)^2 \, dt$$

$$= \tfrac{2}{3} T + T_I - T = T_I - \frac{T}{3}. \tag{9}$$

DELTA NOISE

$$\langle N_\Delta^2 \rangle = \int_0^\infty [R'(t)]^2 \, dt = 2\int_0^T \left(\frac{1}{T^2}\right) dt = \frac{2}{T}. \tag{10}$$

To illustrate the potential value of this type of pulse-shaper we will compare it directly with a simple time-invariant trapezoidal pulse-shaper, using typical values for the time parameters. The following requirements will be placed on each system:

a) Total dead time = 2 μsec (i.e. all signal pulses in the system must return to the baseline in 2 μsec).

b) The duration of the flat-top must be 0.2 μsec.

Using the relationships (5) and (6) for the time-invariant trapezoidal shaper, and (9) and (10) for the gated integrator we have:

Time-invariant trapezoidal shaper	$\langle N_s^2 \rangle = 0.8$, $\langle N_\Delta^2 \rangle = 2.22$;
Gated-integrator trapezoidal shaper	$\langle N_s^2 \rangle = 1.4$, $\langle N_\Delta^2 \rangle = 1.11$.

The gated-integrator delta-noise index is considerably better, and its step-noise index worse than the equivalent quantities for the time-invariant shaper. For short shaping-times, step-noise is usually negligible compared with delta-noise, and the spectral line-width, or at least that part contributed by noise, should be better by a factor of almost $\sqrt{2}$ when the gated integrator is used instead of the time-invariant pulse-shaper. This result is achieved while retaining equally good counting-rate behavior and the same insensitivity to detector signal rise-time. Alternatively, by making

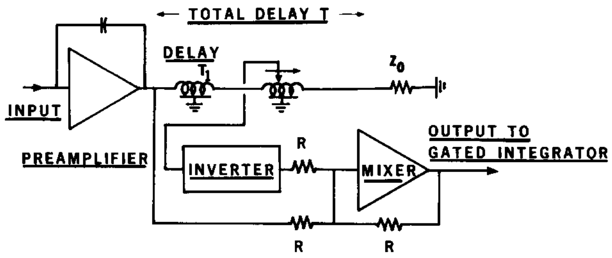

Fig. 6. Example of time-variant differentiator (delay changed from T_1 to T in a very short interval Δt at the start of the signal).

the time-scale of the gated-integrator system one half that used for the time-invariant pulse-shaper, the counting rate performance is improved, while the delta-noise index is the same for the two systems.

Radeka[3]) points out the problems involved in achieving the rectangular pulse-shape used to drive the gated-integrator. To circumvent this difficulty, he uses a Gaussian pulse-shape, produced by a single RC differentiator, and multiple RC integrators, to approximate the rectangular pulse-shape. Analysis of this case is somewhat more laborious, so we will delay it to give consideration to a more sophisticated type of time-variant filter.

4.4. Gated-integrator trapezoidal pulse-shaper with time-variant differentiator

It is interesting to consider a relatively simple modification of the scheme of the previous example: we switch the differentiator that determines the pulse-width into the gated-integrator so that the pulse-width has a small value T_1 when no signal is present, but changes to the value T (as in example 4.3) at the arrival of a signal and until the end of the integration period. At first sight it may appear that the shorter step-noise pulse-width prior to signal arrival might reduce noise, but we will see that this is certainly not so for delta-noise.

We choose to examine this type of system because it has possible value in permitting only short pulses in the amplifier, except when the normal value is necessary for signal processing. If detector pulses are present at a high rate, as during the beam burst of an accelerator, keeping the pulse-widths in the system very short prevents overload and recovery problems. It is therefore important to evaluate the noise penalty paid for switching the pulse-forming circuit.

In this case, it is necessary to discuss the details of the circuit used to shape the square pulse into the gated-integrator. In general, time-variant differentiators must be treated as individual cases, and the analysis must be carried out carefully to avoid pitfalls. General conclusions are difficult to determine, but we have chosen the particular circuit of fig. 6 to illustrate some aspects of switched-differentiator performance. The step-function signal splits into two paths, such that a delayed version of the signal is subtracted from the signal itself to produce the pulse into the gated-integrator. The delay is determined by a delay-line whose value is changed from T_1 when no signal is present to T when a signal occurs. The change in delay is not made instantaneously, but rather over a short time ΔT – assumed to be much smaller than T_1 – the change starting immediately on arrival of the signal.

Fig. 7 shows the various functions appropriate here. Construction of the diagram of the step-noise residual function $R(t)$ is more difficult in this case than in the earlier examples. As we look back from the measurement time T_m, noise steps occurring after the signal arrival time (i.e. within T_I prior to T_m) will be treated exactly as in example 4.3, since they produce pulses of width T into the gated integrator. Due to the delay in delay-line T_1, the same behavior will apply to noise-steps occurring in the interval $(T_1 - \Delta t)$ prior to the start of the signal, since by the time the signal wave reaches the junction of the two delay lines, the signal pick-off point will have moved to the end of the second delay line. However, noise steps occurring prior to the start of the signal by more than T_1 will produce pulses only T_1 long, and they will not overlap the time period

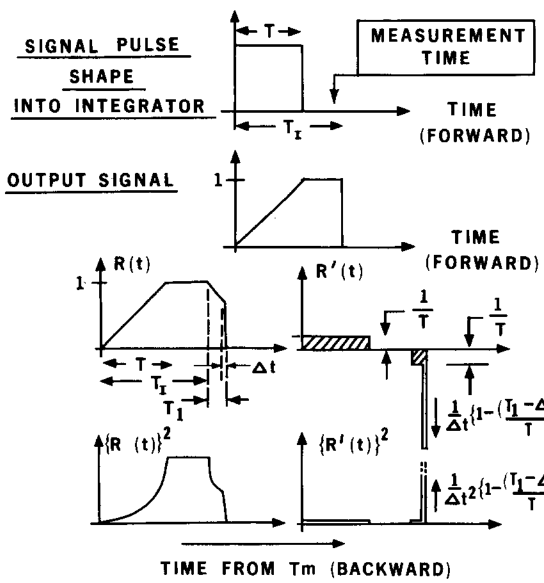

Fig. 7. Gated-integrator trapezoidal pulse-shaper with time-variant differentiator.

when the gated integrator is active. Consequently $R(t)$ is as shown in fig. 7.

Since the area under $R(t)$ is substantially smaller in this case than in case 4.3 (fig. 5), it is clear that the step-noise is better. However, the behavior of $R'(t)$ leads to a large increase in delta-noise (which is particularly important in modern low-noise amplifiers used at short shaping-times). As the total area of $R'(t)$ must be zero, $[R'(t)]^2$ is dominated by the large switching spike in $R'(t)$, which results in a very large increase in delta-noise.

We have:

STEP NOISE

$$\begin{aligned}\langle N_s^2\rangle &= \int_0^\infty [R(t)]^2\,dt \\ &\simeq \int_0^T \left(\frac{t}{T}\right)^2 dt + \int_0^{T_1-T} (1)^2\,dt + \int_{T-T_1}^T \left(\frac{t}{T}\right)^2 dt \\ &\simeq \frac{T}{3} + T_1 - T + \frac{T}{3} - \frac{1}{3T^2}(T-T_1)^3 \\ &= T_1 - \frac{T}{3} - \frac{T}{3}\left(1-\frac{T_1}{T}\right)^3. \end{aligned} \tag{11}$$

DELTA NOISE

$$\begin{aligned}\langle N_\Delta^2\rangle &= \int_0^\infty [R'(t)]^2\,dt \\ &= \int_0^T \frac{1}{T^2}\,dt + \int_0^{(T_1-\Delta t)} \frac{1}{T^2}\,dt \\ &\quad + \int_0^{\Delta t} \frac{1}{\Delta t^2}\left(1-\frac{T_1-\Delta t}{T}\right)^2 dt \\ &= \frac{1}{T} + \frac{T_1-\Delta t}{T^2} + \frac{1}{\Delta t}\left(1-\frac{T_1-\Delta t}{T}\right)^2. \end{aligned}$$

If $\Delta t \ll T_1$, then

$$\langle N_\Delta^2\rangle = \frac{1}{T} + \frac{T_1}{T^2} + \frac{1}{\Delta t}\,\frac{(T-T_1)}{T}.$$

The last term in this expression will normally be dominant, so:

$$\langle N_\Delta^2\rangle \simeq \frac{(1-T_1/T)}{\Delta t}. \tag{12}$$

For example, if $T=1.8\ \mu$sec, $T_1 = 0.2\ \mu$sec, $\Delta t = 50\ n$sec, then

$$\langle N_\Delta^2\rangle \simeq 18.$$

This compares with the value of $\langle N_\Delta^2\rangle = 1.11$ for the simple gated-integrator for $T = 1.8\ \mu$sec and $T_1 = 2\ \mu$sec.

Two aspects of this analysis are of great practical interest:

1) It is clear from the foregoing analysis that the severity of the penalty in delta-noise produced by the time-variant differentiator is proportional to the switching speed of the differentiator (i.e. $\propto 1/\Delta t$). In practice, slow changes of circuit parameters are not easy to achieve. However, a little thought about the function $R(t)$ shows that we can achieve the same effect by using a RC integrator in the circuit preceeding the differentiator. Therefore, even if the differentiator is switched instantaneously, integration in the early stages limits the increase in delta-noise.

2) Possibly the major interest in switched-differentiators occurs in pulsed-beam accelerator applications, where reducing the differentiation time prevents overload, and speeds-up recovery following the end of the beam pulse. In this case, the differentiator may be switched to its normal value T at the end of the beam burst. It is then of interest to determine the time period following this operation during which a noise penalty occurs. A little thought about the function $R(t)$ shows that the penalty diminishes steadily for a time T after the end of the beam burst, and that noise performance for signals starting at times later than T after the end of the burst is the same as for the simple gated-integrator system.

4.5. Biphase-pulse followed by a gated integrator

In case 4.1 we considered a time-invariant trapezoidal pulse-shaper. The symmetrical triangle can be considered as a special case of this, and its noise indices, derived from eqs. (3) and (4) by substituting $\tau_2 = 0$, $\tau_1 = \tau_3 = \tau$, are:

$$\langle N_s^2\rangle = \tfrac{2}{3}\tau, \tag{13}$$

$$\langle N_\Delta^2\rangle = 2/\tau, \tag{14}$$

where τ = the peaking time of the triangle.

This triangular response can be obtained by developing a biphase pulse with each half having a duration τ, and feeding it into an integrator. The signal response remains the same whether the integrator is in continuous operation or is opened only for the duration of the biphase pulse, but the noise behavior expressed by eqs. (13) and (14) applies only to the ungated integrator. The noise performance is quite different when the integrator is switched in only for the signal time,

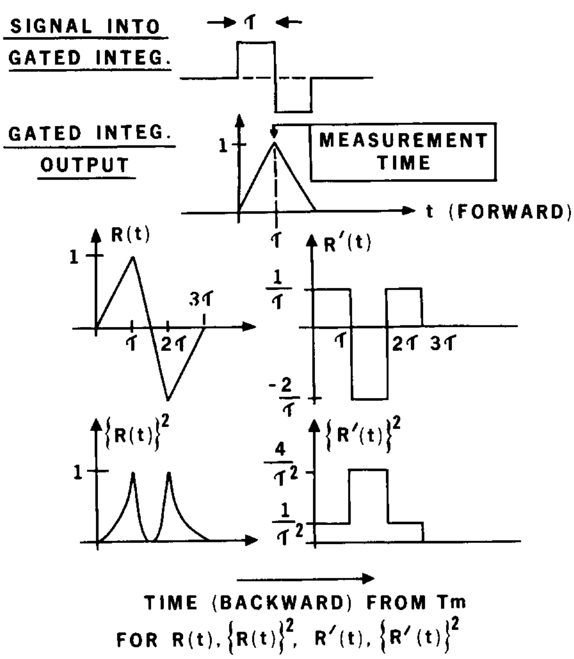

Fig. 8. Biphase pulse followed by a gated-integrator.

despite the fact that the final output signal looks precisely the same.

Fig. 8 shows $R(t)$, and the derived functions, for the case of the switched integrator. We have:

STEP NOISE

$$\langle N_s^2\rangle = \int_0^\infty [R(t)]^2 \mathrm{d}t = 2\int_0^\tau \left(\frac{t}{\tau}\right)^2 \mathrm{d}t + 2\int_0^{\tau/2} \left(\frac{2t}{\tau}\right)^2 \mathrm{d}t$$

$$= \frac{2\tau}{3} + \frac{\tau}{3} = \tau. \tag{15}$$

DELTA NOISE

$$\langle N_\Delta^2\rangle = \int_0^\infty [R'(t)]^2 \mathrm{d}t = \frac{2}{\tau} + \frac{4}{\tau} = \frac{6}{\tau}. \tag{16}$$

Comparing these results with eqs. (13) and (14), it is apparent that the switching operation associated with the gated-integrator has substantially degraded both step- and delta-noise. This result has been presented to show that care must be exercised in changing circuit parameters in synchronism with signals, or a severe penalty in noise may result.

5. Digital calculations of more complex cases

The analysis technique described here involves only very simple integrations in the time domain, and the integrations can readily be broken down into convenient pieces as illustrated in the examples in the previous section. These examples were chosen to use relatively simple pulse-shapes to simplify the description of the technique, but the method can equally well be applied to a very wide range of pulse-shapes, including those expressible in analytical form (e.g. example 4.2), and those that can be expressed only as a table of amplitude vs time. No limitation exists due to discontinuities in waveforms. Integrations can frequently be carried out by normal analytical methods, but it is particularly convenient to use the power of digital computers to perform many of the more laborious integrations.

It is necessary to program the noise calculations differently depending upon whether the system is time-invariant, or is a gated-integrator or a more complicated time-variant system. However, once such a program is written, it can handle a wide range of basic signal shapes. The structure of the program required to handle the gated-integrator system will be described in the following paragraphs using the illustration of fig. 9. The step-by-step procedure followed in this calculation duplicates the mental procedures involved in forming $R(t)$; as such, it may serve to review the method for those readers who encountered problems in constructing $R(t)$ in the foregoing examples.

The program requires that an array of N locations be loaded with N values representing the signal amplitude entering the gated-integrator in each of N equal

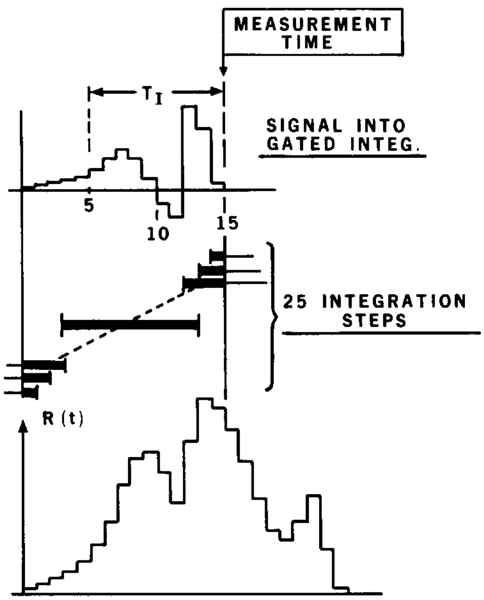

Fig. 9. Illustrating the steps involved in a gated-integrator system analysis program.

time intervals Δt. The total time-span represented by the array (i.e. $N\Delta t$) must cover all significant parts of the signal. The array may be loaded manually in cases where the waveform cannot be represented as a sequence of analytical functions, or loaded by sub-programs if analytical representations are possible. In fig. 9, the top diagram represents the values loaded into the array – in this case only 15 locations (i.e. $N = 15$) are used, but a much larger number is used in practice.

The program also requires knowing the integration time T_I used in the gated integrator. For the purpose of the calculation, T_I is considered as N_I intervals each of Δt duration. In fig. 9, N_I is 10.

The first main sequence in the program consists of establishing a new data-array with $N_I + N$ elements representing the step-noise residual function $R(t)$. To do this, the integration interval is, in effect, slid over the signal waveform, one step at a time, from just overlapping the start of the signal waveform to just overlapping its end (see fig. 9). At each step, digital integration of the signal waveform over the signal intervals within the integration period is carried out, and the result is stored in the appropriate location in the $R(t)$ array. After $N + N_I$ steps, the $R(t)$ array is fully loaded.

Once the $R(t)$ array is loaded, it is simple to carry out the digital integration of $[R(t)]^2$ over the full span of $R(t)$ while leaving the $R(t)$ array undisturbed. After this operation, the value of the integral of $[R'(t)]^2$ is caculated by performing the summation of $[R(t_n+1) - R(t_n)]^2$. Finally, the integral S of the signal waveform over the interval T_I is calculated, the values of $[R(t)]^2$ and $[R'(t)]^2$ are divided by S^2, and the appropriate time normalization is applied to give the step- and delta-noise indices.

Programs have been developed for several shaping systems, and noise indices have been calculated. Fig. 10 shows the values obtained for many types of shaper, including some of the examples used in our earlier description. We will now discuss some of these results.

PULSE-SHAPES	OUTPUT SIGNAL	$<N_S^2>$	$<N_\Delta^2>$
1. R C INTEG.-DIFF. (TIME-INVARIANT)	τ_0	$1.87\,\tau_0$	$1.87/\tau_0$
2. TRAPEZOID (TIME-INVARIANT)	τ_1 τ_2 τ_3	$\tau_2 + \frac{\tau_1+\tau_3}{3}$	$\frac{1}{\tau_1} + \frac{1}{\tau_3}$
3. TRAPEZOID: SQUARE PULSE (T) INTO GATED INTEGRATOR (T_I)	T T_I	$T_I - \frac{T}{3}$	$2/T$
4. TRIANGLE: BIPHASE PULSE INTO GATED INTEGRATOR	τ_0	τ_0	$6/\tau_0$
5. GAUSSIAN $X^7e^{7(1-X)}$ (TIME-INVARIANT)	τ_0	$0.67\,\tau_0$	$2.53/\tau_0$
6. GAUSSIAN $X^7e^{7(1-X)}$ INTO GATED INTEGRATOR	T_I $T_I = 2.5\,\tau_0$	$2.07\,\tau_0$	$1.47/\tau_0$
7. GAUSSIAN $X^4e^{4(1-X)}$ (TIME-INVARIANT)	τ_0	$0.90\,\tau_0$	$2.04/\tau_0$
8. R C DIFF. ($\tau_0/3$) INTO GATED INTEGRATOR ($T_I=\tau_0$)	$T_I=\tau_0$	$0.89\,\tau_0$	$1.87/\tau_0$
9. TRIANGLE, AUTO-CORRELATED THEN INTO GATED INTEGRATOR $T_I=2\,\tau_0$; $\tau_0=\Delta$PEAK	T_I	$1.08\,\tau_0$	$1.48/\tau_0$
10. GAUSSIAN, AUTO-CORRELATED THEN INTO GATED INTEGRATOR $T_I=2\,\tau_0$, τ_0=GAUSSIAN PEAK	T_I	$0.92\,\tau_0$	$1.66/\tau_0$
11. TRAPEZOID: SQUARE PULSE INTO GATED INTEGRATOR, PULSE WIDTH SWITCHED FROM T_1 TO T IN Δt AT START OF SIGNAL	T_I	$T_I - \frac{T}{3} - \frac{T}{3}\left(1-\frac{T_1}{T}\right)^3$	$\frac{\left(1-\frac{T_1}{T}\right)}{\Delta t}$

Fig. 10. Summary of noise indices for typical systems.

6. Perspective on pulse-shapers

The results given in fig. 10 include a number of time-invariant shapers (1, 2, 5, 7), combinations of these with gated-integrators (3, 4, 6, 8), with a switched differentiator (11), and examples of autocorrelation of the signal combined with gated-integrator (9, 10). In these latter cases, the signal was processed by carrying out the integration:

$$\int_0^T S(t)\cdot S_0(t)\,\mathrm{d}t,$$

where

T is the total signal duration.

$S(t)$ is the signal (processed by the appropriate network).

$S_0(t)$ is a reference waveform whose shape is the same as the signal, triggered to start at the same time as it.

As this method appears to give greatest weight to information when the signal has its maximum value, intuition suggests that some improvement in signal/noise might result. The fast analogue-multiplication required for pulse-shaping of this type to be feasible can now be performed if justified by signal/noise performance improvements.

The intriguing simplicity of these noise calculations tends to hide the fact that correct choice of a pulse-shaper for a given application depends on good judgement between a variety of partially conflicting requirements, and also requires a knowledge of the engineering problems involved in achieving a certain pulse-shape. Injection of some of these factors is necessary if the results given in fig. 10 are to be useful. To re-emphasize the various important factors, we restate them here from an earlier section of the paper:

1) Signal/noise performance.
2) Counting-rate behavior.
3) Sensitivity of output pulse-amplitude to rise-time fluctuations in the detector signal.
4) Suitability of output-pulse for feeding a pulse-height analyzer.

And we add:

5) The pulse-shape must be realizable with simple circuits using elements that do not introduce signal distortions of an undesirable nature.

Noise analysis is directed only at item (1), but intimately involves item (2) as the duration of any waveform in the system directly determines the probability of pulse pile-up at high counting-rates. Item (3) requires a pulse-shape possessing a flat (or nearly flat) top for a time greater than the maximum detector signal rise-time variation. For many applications, however, detector signal rise-time fluctuations are negligible, and need not be considered as an important factor in the choice of pulse-shaper. Item (4) also requires a flat-topped pulse, although the use of pulse-stretchers capable of responding to narrow pulses generally makes this factor of minor importance. The final item (5) is a complex one involving considerable knowlegde of circuit elements. However, one major consideration relates to delay-lines – the only circuit elements capable of producing rectangular pulses, and therefore a necessary component if several of the pulse-shapes of fig. 10 are to be realized. While delay-lines are useful in many applications, their deficiencies limit their use to non-critical systems. Critical systems are better realized using stable components like resistors and capacitors – even inductors should be avoided due to their imperfections, including temperature instability.

Examination of the results in fig. 10 confirms, in every case, that the step-noise index is proportional to the time-scale of the pulse-shaper, while the delta-noise index is inversely proportional to it. Choice of the actual time-scale depends on the relative sizes of the sources of step- and delta-noise (n_s and n_Δ). Ideally, if delta-noise is dominant at a given time-scale, the time-scale can be lengthened to reduce delta-noise until the step-noise (which is increasing for larger time-scales) becomes equal to it. On this basis, an optimum time-scale can be achieved for each type of shaper. In many cases, however, this is an impractical procedure as the time-scale required to achieve equality of delta- and step-noise is very long, and the resulting pile-up problems at high counting-rates are intolerable. Therefore, the main emphasis in choosing a pulse-shaper is usually to choose that shaper giving the best delta-noise, while restricting the time-duration of any signal in the system to an acceptable value from the point of view of counting rate.

The results of fig. 10 are best appreciated by comparing some of the cases. For example, the traditional single-RC integrator – differentiator combination (1) appears at first sight to exhibit superior delta-noise performance to that exhibited by the 7th- or 4th-order Gaussian shapes*, since the calculated value of $\langle N_\Delta^2 \rangle$ is greater in cases (5) and (7) than in case (1). However, the long tail on the waveform of (1), compared with either (5) or (7), causes severe signal pile-up effects at high counting-rates. For this reason a larger value of τ_0 can be used with (5) or (7) than with (1), thereby reducing the delta-noise well below that of case (1), while retaining an adequate value of $\langle N_s^2 \rangle$. This is one example of a general rule for time-invariant systems, namely that symmetrical waveshapes always result in less delta-noise than asymmetrical ones when equal recovery times are demanded of both. On these grounds, the 7th order Gaussian is preferred over the 4th order Gaussian, but the increased circuit complexity needed for the former case may not be considered to be justified.

Another useful comparison is that between a gated-integrator fed by a Gaussian-shaped pulse (6), and the Gaussian-shaper with no gated-integrator (5). A number of interesting features emerge from this comparison:

1) The counting-rate behavior will be the same if the same value of the Gaussian peaking-time is used.

2) Delta-noise is significantly better for the gated-integrator, but the step-noise is worse. Where delta-noise is dominant, an improvement in signal/noise can be realized by using the gated-integrator.

3) The nearly flat region at the measurement time of the gated-integrator output makes the output insensitive to detector signal rise-time fluctuations. The integration period T_1 can readily be chosen to produce an adequately flat-top to cope with any reasonable amount of rise-time fluctuation in the detector signal. As shown by Radeka[3]), this feature makes this type of shaper very attractive for high-energy γ-ray spectroscopy using large germanium detectors.

We have already compared the behavior of the

* These shapes are produced by 1 RC differentiator and 7 or 4 RC integrators respectively.

switched-differentiator-shaper (11) with that of the gated-integrator (3), and have shown that a severe delta-noise penalty results from the switching operation. Despite this, as was shown earlier, the switched differentiator can be useful in circumstances that arise in pulsed-beam accelerator experiments.

Finally, comparison of cases (10) and (6) indicates some possible value in the auto-correlation method. The auto-correlation shaper (10) is substantially better in its step-noise performance, while exhibiting almost the same delta-noise performance as the gated-integrator (6). In systems where step-noise is a serious factor, the benefits of the auto-correlation method may justify the circuit complexity required for its execution. At the present time, no system of this type is in use, and the possible difficulties of analogue multiplication have not been evaluated.

7. Conclusion

The simplicity of noise calculations using this method has been clearly demonstrated here. For the unbeliever, we recommend an attempt to carry out similar calculations by the time-honored method of Fourier-transforming the waveforms, and integrating in the frequency domain. Furthermore, the older methods are unable to deal with time-variant systems, whereas they can be handled relatively easily using the new technique. A number of practical advantages and disadvantages of the time-variant methods are pointed out in the text.

It appears that the analysis technique should find much wider application, particularly as it provides clear pictures of the basic resasons for superior or inferior performance of systems. Perhaps the simplicity of the method, and the physical basis for the calculations, will encourage physicists to realize that there are sound reasons for the various techniques employed to optimize pulse-shapes in amplifiers used for nuclear experiments.

It is a pleasure to acknowledge many discussions with D. Landis, J. Walton, B. Leskovar, and particularly those with V. Radeka. Stimulation for writing this account came from conversations with physicists baffled by the supposed "recipes" of engineers; J. Jaklevic and R. Pehl must bear some responsibility in this regard.

This work was carried out as part of the program of the Nuclear Chemistry Division of the Lawrence Berkeley Laboratory supported by the U. S. Atomic Energy Commission Contract No. W-7405-eng-48.

References

[1]) G. Amsel, R. Bosshard and C. Zajde, IEEE Trans. Nucl. Sci. NS-**14**, no. 1 (1967) 1.

[2]) V. Radeka and N. Karlovac, Time-variant filters, in *Semiconductor radiation detectors and circuits*, Nat. Acad. Sci. Publ. 1593 (1969) p. 553.

[3]) V. Radeka, Trapezoidal filtering of signals from large germanium detectors at high rates, BNL-16245 (1971); IEEE Trans. Nucl. Sci. NS-**19** (Feb. 1972).

[4]) M. O. Deighton, Calculation of noise/signal ratio of a nuclear pulse amplifier employing gated active integration, AERE Report R5021 (1967).